



HAL
open science

Redox reactions of $\text{K}[\text{Fe}(\text{CN})]$ during mechanochemically stimulated phase transitions of AlOOH

Reinhard Stösser, Michael Feist, Kerstin Patzwaldt, Michael Menzel,
Franziska Emmerling

► **To cite this version:**

Reinhard Stösser, Michael Feist, Kerstin Patzwaldt, Michael Menzel, Franziska Emmerling. Redox reactions of $\text{K}[\text{Fe}(\text{CN})]$ during mechanochemically stimulated phase transitions of AlOOH . *Journal of Physics and Chemistry of Solids*, 2011, 10.1016/j.jpcs.2011.03.016 . hal-00753044

HAL Id: hal-00753044

<https://hal.science/hal-00753044>

Submitted on 17 Nov 2012

HAL is a multi-disciplinary open access archive for the deposit and dissemination of scientific research documents, whether they are published or not. The documents may come from teaching and research institutions in France or abroad, or from public or private research centers.

L'archive ouverte pluridisciplinaire **HAL**, est destinée au dépôt et à la diffusion de documents scientifiques de niveau recherche, publiés ou non, émanant des établissements d'enseignement et de recherche français ou étrangers, des laboratoires publics ou privés.

Author's Accepted Manuscript

Redox reactions of $K_3[Fe(CN)_6]$ during mechanochemically stimulated phase transitions of AIOOH

Reinhard Stöber, Michael Feist, Kerstin Patzwaldt, Michael Menzel, Franziska Emmerling

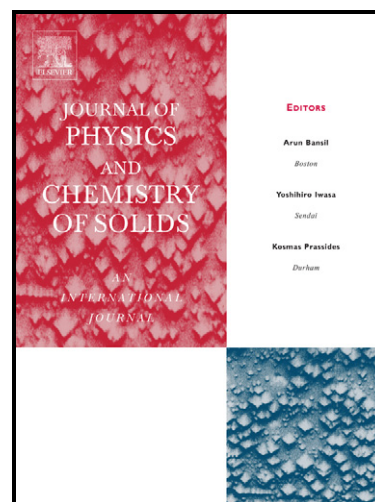
PII: S0022-3697(11)00071-0
DOI: doi:10.1016/j.jpacs.2011.03.016
Reference: PCS 6437

To appear in: *Journal of Physics and Chemistry of Solids*

Received date: 15 November 2010
Revised date: 5 March 2011
Accepted date: 25 March 2011

Cite this article as: Reinhard Stöber, Michael Feist, Kerstin Patzwaldt, Michael Menzel and Franziska Emmerling, Redox reactions of $K_3[Fe(CN)_6]$ during mechanochemically stimulated phase transitions of AIOOH, *Journal of Physics and Chemistry of Solids*, doi:10.1016/j.jpacs.2011.03.016

This is a PDF file of an unedited manuscript that has been accepted for publication. As a service to our customers we are providing this early version of the manuscript. The manuscript will undergo copyediting, typesetting, and review of the resulting galley proof before it is published in its final citable form. Please note that during the production process errors may be discovered which could affect the content, and all legal disclaimers that apply to the journal pertain.



www.elsevier.com/locate/jpcs

Redox reactions of $\text{K}_3[\text{Fe}(\text{CN})_6]$ during mechanochemically stimulated phase transitions of AlOOH

Reinhard Stößer¹, Michael Feist^{1*}, Kerstin Patzwaldt¹,
Michael Menzel², and Franziska Emmerling²

¹ Institut für Chemie der Humboldt-Universität zu Berlin, Brook-Taylor-Straße 2,
D-12489 Berlin, Germany, E-mail: feistm@chemie.hu-berlin.de

² Bundesanstalt für Materialforschung und -prüfung, Richard-Willstätter-Straße 11,
D-12489 Berlin, Germany, E-mail: franziska.emmerling@bam.de

* Corresponding author, Phone: (+49) 30 2093 7346, Fax: (+49) 30 2093 7392

Abstract

Thermally induced redox reactions of $K_3[Fe(CN)_6]$ (**1**) were investigated for a broad temperature range by thermal methods and structure analytical methods (ESR and Mößbauer spectroscopy, X-ray Powder diffraction and XANES). Based on the influence of the mechanically activated and transforming matrices **2** and **3**, redox processes can be tuned to form doped Al_2O_3 systems which contain either isolated Fe^{3+} centres or redox active phases and precursors like $(Al_{1-x}Fe_x)_2O_3$ (**4**), $(Al_{3-x}Fe_x)O_4$ (**5**), Fe_3O_4 , Fe_2O_3 and Fe^0 . The phase Fe_3C and the chemically reactive C-species were detected during the reaction of **1**. The final composition of the doped products of α - Al_2O_3 is mainly influenced by the chemical nature of the Fe doping component, the applied temperature and time regime, and the composition of the gas phase (N_2 , N_2/O_2 or N_2/H_2). From the solid state chemistry point of view it is interesting that the transforming matrix (**2**, **3**) possesses both oxidative and protective properties and that the incorporation of the Fe species can be performed systematically.

Key words: ESR and Mößbauer spectroscopy · Mechanical activation · Potassium hexacyanoferrate(III) · Redox reactions · TA-MS measurements · XRD

1. Introduction

Potassium hexacyanoferrate(III), $K_3[Fe(CN)_6]$ (**1**), continues to be a chemical „evergreen“ which is also true for *Berlin Blue*. This could be deduced, last but not least, from the observation of a never ending stream of reports on novel chemical and application aspects found for **1**. The present paper contributes to this by reporting some unexpected spectroscopic and chemical findings which were obtained by a combination of thermal and spectroscopic investigations of **1** in the form of the pure substance as well as after mechanochemically performed doping of AlOOH xerogels (**2**) with **1** and other Fe species, followed by a thermal treatment.

The aim of this study is deduced from the question whether a targeted Fe doping of Al_2O_3 samples could be realized by combining the competing mechanochemically and thermally stimulated redox processes of iron with the transformation processes occurring within an AlOOH/ Al_2O_3 matrix. This question is closely related to the preparation of supported aluminium oxide catalysts with a defined Fe^{II} or Fe^{III} content, as well as to the preparation of magnetic

materials [1-3] by primarily employing the chemical properties of the Al_2O_3 precursors and the special properties of their AlO_x matrices.

A first and important step concerning the investigation of the thermal decomposition of **1** was given by Wolski *et al.* [4-5]. Based on careful chemical analysis and long term thermal analysis, the authors determined the structures of several intermediates. The investigations described here support the results of the authors concerning pure **1**, but include additional findings. The synthesis and structural characterisation of the pure crystalline phases of ternary and quaternary metal nitrides [6], carbides [7] and carbometallates [8] and their thermochemistry [9] is well documented in the literature and contain numerous novel and unique results. The approach is comparable to that followed in the current publication. Here, however, we focused on a more phenomenological description with regard to the redox processes of **1** competing with the chemistry of the $\text{AlO}(\text{OH})$ matrix transformation.

2. Results and Discussion

The investigation of the thermal behaviour of pure **1** by employing a thermal analyzer simultaneously coupled to a mass spectrometer (TA-MS) is depicted in Figure 1a together with the results of the characterization of separately tempered (0.5 h/N_2) samples corresponding to the essential stages of the thermanalytical (TA) curves obtained during the linear heating run. The thermal activation causes an internal redox process in **1** that results in the liberation of $(\text{CN})_2$ and to the formation of lower-valent Fe species. In this concern, the good agreement of the TA-MS findings (Figure 1a) to the Mößbauer data is obvious. They were confirmed and completed by the results of the X-ray powder diffraction (XRD), the X-ray absorption near edge spectroscopy (XANES), and the electron spin resonance (ESR) spectroscopy (Supporting information in S1 - S5). Stable intermediates being formed in defined temperature-time ranges could be identified (Figures 1b, 1c) and allow description of the evolution of the Fe_3C and Fe^0 product phases. The thermal process is accompanied by colour changes starting with yellow, followed by greenish-blue to black.

Furthermore, one can deduce from Figure 1 that the thermally initiated reactions start above $250 \text{ }^\circ\text{C}$ and that the well separated mass loss around $300 \text{ }^\circ\text{C}$ is caused by the exothermal (peak temperature T_p $338 \text{ }^\circ\text{C}$) release of $(\text{CN})_2$ and, to a minor extent, of HCN. This is accompanied by the formation of Fe^{II} species in the solid residue, which is clearly indicated by the results of the Mößbauer investigations together with XRD and XANES (cf. S2 - S4). The

XANES measurements were especially helpful in the case of sample **1** tempered at 300 °C. Here, the formation of Fe^{II} was indicated by the Mößbauer data, but could not be confirmed by XRD due to a low crystallinity of the solid phase formed. It could be shown by XANES, however, that 21 % Fe^{II} was contained in the sample with, expectedly, a major part of Fe^{III} (cf. S4). It is obvious that structurally distorted precursors of *Berlin Blue* were formed [10-11]. In the following temperature range between 400 and 650 °C, however, significant changes could not be established neither by thermal nor by spectroscopic methods. In the solid residues, K₄[Fe(CN)₆] is contained, as could be evidenced by XRD. Above 700 °C, on the other hand, Fe₃C is unambiguously detected both by Mößbauer spectroscopy and XRD, even if K₄[Fe(CN)₆] remains to be the major component of the product phase.

Above 900 °C, metallic Fe⁰ can be detected unambiguously in the solid residue (Figure 1b, c); it is coexisting with KHCO₃ (cf. S3a), which is unusual, but in line with the mass spectrometric detection of CO₂. This formation of carbonate or CO₂ can be explained by highly reactive carbon formed within the decomposing matrix of **1** and is obviously able to react with oxygen traces in the carrier gas.¹

After the final tempering of **1** under N₂ at 1100 °C, the phases α-Fe und Fe₃C (Cohenite) could be detected by XRD which directly supports the Mößbauer findings (Figure 1, cf. also S2c) and is in line with the ESR data, i.e. the ferromagnetic resonances.

As a mechanism for this kind of “self-reduction” of **1**, a reaction sequence can be proposed that begins with the release of (CN)₂, is then followed by transformations yielding Fe^{II}₃(CN)₆, and ends up with the formation of α-Fe, Fe₃C, and C (Figure 2). This would be both a support and a substantial extension of the decomposition mechanism proposed by Raj and Danor [12].

A completely different decomposition proceeds if untreated **1** is mixed with a mechanically activated (50 h *high-energy ball milling*), originally crystalline AlOOH (**3**), then co-milled for further 8 h, and subsequently subjected to a TA heating run (Figure 3a). The TA-MS curves of the mixture {30% **1** + 70% **3**} and the Mößbauer spectrum of the residue after 1200 °C under N₂ in Figure 3 clearly show that the intermediates formed from **1** react with the transforming matrix **3**. A certain similarity with the TA-MS curves in Figure 1 might be deduced,

¹ Measurements with an oxygen sensor (Dr. J. Hanss, University of Augsburg, Germany) yielded an oxygen content in the inert gas (Ar, N₂) of ca. 80 ppm. A comparing TA-MS measurement of non-milled Fe powder under N₂ and the same conditions as applied for **1** exhibited no mass gain at all, i.e. oxidation does not occur under these conditions.

but undoubtedly no $(\text{CN})_2$ is formed here and, as before, a low quantity of HCN (200-500 °C) is released. Furthermore, the water release from **3** starts earlier (ca. 160 °C) than in the case of matrix **2**, but is intense and spread over a large temperature range up to 500 °C as does HCN.

The Mößbauer spectrum of the residue of the TA run comprises two sextets caused by 62.1 % Fe^0 and 15.4 % Fe_3C , respectively, and one singlet (22.5 %) showing a comparably small isomer shift (IS) that has to be related to Fe^{III} (cf. S2). This Fe^{III} species was formed by an oxidative reaction of **1** with the matrix **3**, even if internal reduction processes of **1** are still predominating in this concentration range (30% **1**).

If the concentration of **1** in the mixture with matrix **3** is lowered, e.g. down to 1 wt-% such as when applied for the study on the transformation of AlOOH xerogels yielding $\alpha\text{-Al}_2\text{O}_3$ [13], the reactive interaction of the intermediates with the matrix is more strongly expressed. The formation of Fe_3C or Fe^0 under N_2 , for instance, is not detectable any more. Figure 4 depicts schematically the experimental approach to yield the mentioned results.

From a mechanochemical point of view it is of particular importance to know that the influence of doping with **1** is weak, even negative concerning the down-shift of the crystallization temperature T_p (formation of $\alpha\text{-Al}_2\text{O}_3$). Compared with the average value of the T_p decrease of 10.9 % (see Table 1), one reaches here only ~20 % of the activation effect being related to the *undoped* matrix. This means that the crystallization starting from the surface of the activated xerogels is blocked by **1** and its decomposition products. This effect, which might be regarded as a mechanochemical deactivation, could be achieved with other dopants as well (cf. S5) which were unable to form appropriate crystallization seeds such as, for example, Fe_2O_3 . Up to now, this kind of a netto activation effect is expressed in the strongest manner in the case of **1** and has to be attributed to its specific thermochemical behaviour, including the reaction with the matrix.

The investigation of several reference systems (Figure 5) allowed it to be demonstrated that (i) the results presented here can be generalized to some extent, (ii) which kind of redox processes occur in the systems, and (iii) how these redox reactions can be influenced by the chemical nature of the Fe^{3+} dopant.

As emphasized by Figure 5, promising possibilities exist for the reactive doping of Al_2O_3 matrices. The surface enrichment of the $\alpha\text{-Al}_2\text{O}_3$ crystallites with the phase precursors $(\text{Al}_{1-x}\text{Fe}_x)_2\text{O}_3$ (**4**) and $(\text{Al}_{3-x}\text{Fe}_x)\text{O}_4$ (**5**) [14], symbolized in Figure 5 by Fe^{3+} or Fe^{2+} respectively, is possible due to competing processes initiated by the type of Fe ligand, the oxidative power of the

transforming AlOOH matrix, as well as the chosen gas atmosphere in the TA runs (cf. especially S1b, integrals in the range of 330 mT).

Interesting results were obtained after the doping of **2** with Fe₃O₄, Fe₂O₃, or Fe⁰. In this concern, the comparably large variation of the Fe⁰ fraction of the total Fe content in the product α -Al₂O₃ is noteworthy. This fraction decreases down to ~50 % in the case of reactive interaction with the matrix, whereas one obtains 100 % Fe⁰ for pure **1** under N₂/10%H₂. If the internal oxidative processes were reinforced by employing Fe(NO₃)₃·9H₂O, despite the forming gas atmosphere, N₂/10%H₂, the Fe⁰ content can be lowered down to ~40 %.

Finally the addition of Fe⁰ powder to **2**, proves that, indeed, the oxidation during interaction with the transforming matrix **2** proceeds stepwise. This is a further support of the proposed interpretation of the findings obtained for the systems {**1**/Matrix}. In fact, the formation of 59 % Fe^{II} and even 21 % Fe^{III} due to oxidation by the matrix (i.e. by in situ liberated water) could be observed after co-milling of **2** with 1 wt-% Fe⁰ and subsequent TA heating run under N₂. Besides these Fe^{II} or Fe^{III} species, protected inside the matrix in the form of the phase precursors **4** and **5**, the coexisting phase Fe₃O₄ being detected exclusively under these conditions was formed as an alternative to the incorporation in the Al-rich phases.

The mechanochemical reactions of the matrix are not restricted to thin layers of the surface region only. XRD studies on mixtures of pre-heated samples of **1** (30 min at 200, 400, 700, 900 °C under N₂, respectively) and **3** demonstrated that the formation of structurally distorted corundum can be evidenced already before tempering (cf. ESR results in S1) which means that parts of the bulk matrix were transformed *mechanochemically*. Corundum particles formed this way are capable to act as seeds for the crystallization of the entire sample and hereby influences the peak temperature T_p of the DTA effect as well (see Table 1). This is in line with the observed ESR signals at $g' \sim 4.3$ [15] which, during the subsequent tempering step, change into the typical Fe^{III}-ESR fine structure for α -Al₂O₃:Fe³⁺ with $g' \sim 13$ and 5.2 [13, 16-17] thus indicating a more pronounced ordering of the structure. Furthermore, the protective (i.e. trapping) function of the matrix for the incorporated Fe^{II} and Fe^{III} species could be evidenced by the ESR data (cf. S1).

3. Conclusions

Summarizing the presented findings, it should be emphasized that they represent (a) the evidence of intermediates of the thermal transformations of **1**, (b) the demonstration of both the

oxidative and protective function of the thermally transforming matrix **2**, together with (c) the oxidative and disperse incorporation of Fe^{3+} ions into the forming $\alpha\text{-Al}_2\text{O}_3$ matrix, (d) the proof of the coexistence of phases with various desired oxidation states of iron, and finally, (e) the demonstration of netto effects causing the decrease of the crystallization temperatures of $\alpha\text{-Al}_2\text{O}_3$ after mechanical activation of mixtures of **2** with Fe^{III} or Fe^0 species.

The choice of the doping component together with an appropriate temperature-time regime, as well as the required composition of the gas phase during the TA heating runs allows either distinct product phases originating from the doping component with particular local magnetical properties (i.e. Fe^0 , Fe_2O_3 , Fe_3O_4 , etc.) to be obtained or to force the incorporation of Fe^{x+} into the phase precursors such as **4** or **5** up to the $x\text{-Al}_2\text{O}_3$ phases ($x=\alpha,\gamma$) which would be a result of the surface-constituting influence of the transforming AlO_x matrix.

4. Experimental

All chemicals were of analytical purity (p.A.) and used as commercially available: $\text{K}_3[\text{Fe}(\text{CN})_6]$ (Laborchemie Apolda, Germany), AlOOH (Nabaltec, USA).

The thermal behaviour was investigated by employing a simultaneously coupled TA-MS device (Netzsch STA 409 C *Skimmer*[®] with a mass spectrometer Balzers QMG 421) in various gas atmospheres (Details in S5). The mechanical activation was performed using a planetary ball mill *Pulverisette* (Fritsch, Germany; details in S7). The ESR spectra were recorded on an X-Band spectrometer (ZWG-Magnettech GmbH, Berlin-Adlershof, Germany) with $\text{MgO}:\text{Cr}^{3+}$ as a standard both for intensity and g' values ($g'=1,9796$). The Mößbauer spectra were obtained with a Wissel Electronics spectrometer (Starnberg, Germany) at 295 and 77 K, respectively. All spectra were normalized to the standard $\alpha\text{-Fe}$ foil (GoodFellow, USA, details in S2). Details about the XRD and XANES measurements can be taken from S3 and S4.

Received:

Published online:

References

- [1] N. Hayashi, I. Sakamoto, H. Tanoue, H. Wakabayashi, T. Toriyama, *Hyperfine Interact.* 141 (2002) 163.
- [2] R. A. Stukan, A. G. Knizhnik, V. E. Prusakov, A. L. Buchachenko, M. M. Levitskii, A. A. Zhdanov, *J. Struct. Chem.* 32 (1991) 830.
- [3] A. L. Buchachenko, *Russ J. Phys. Chem.* 83 (2009) 1637.
- [4] W. Wolski, B. Porawski, *J. Therm. Anal.* 7 (1975) 139.
- [5] W. Wolski, B. Porawski, *J. Therm. Anal.* 9 (1976) 181.
- [6] R. Kniep, *Pure Appl. Chem.* 69 (1997) 185.
- [7] B. Davaasuren, H. Borrmann, E. Dashjav, G. Kreiner, M. Widom, W. Schnelle, F. R. Wagner, R. Kniep, *Angew. Chem. Int. Edit.* 49 (2010) 5687.
- [8] E. Dashjav, G. Kreiner, W. Schnelle, F. R. Wagner, R. Kniep, W. Jeitschko, *J. Solid State Chem.* 180 (2007) 636.
- [9] A. Gudat, R. Kniep, A. Rabenau, *Thermochim. Acta* 160 (1990) 49.
- [10] B. Mohai, L. Bagyin, *J. Inorg. Nucl. Chem.* 33 (1971) 3311.
- [11] M. Verdaguev, G. S. Girolami, in : *Magnetism: Molecules and Materials* (Eds.: J. S. Miller, M. Drillon), VCH, Weinheim, 2005, pp. 284.
- [12] D. Raj, J. Danon, *J. Inorg. Nucl. Chem.* 37 (1975) 2039.
- [13] M. Nofz, R. Stöber, G. Scholz, I. Dorfel, D. Schultze, *J. Eur. Ceram. Soc.* 25 (2005) 1095.
- [14] R. Stöber, M. Menzel, M. Feist, *Hyperfine Interact.* 190 (2009) 43.
- [15] R. Stöber, G. Scholz, J. Y. Buzaré, G. Silly, M. Nofz, D. Schultze, *J. Am. Ceram. Soc.* 88 (2005) 2913.
- [16] R. Stöber, M. Feist, *J. Phys. Chem. C* 112 (2008) 16438.
- [17] R. Stöber, M. Feist, M. Menzel, M. Nofz, *J. Am. Ceram. Soc.* 93 (2010) 1447.

Supplementary information (S1 - S6) is available in the www under <http://www.sciencedirect.com> or directly from the author.

Figure captions

Figure 1

- (a) TA-MS curves of $K_3[Fe(CN)_6]$ (**1**) (34,89 mg) in N_2 with the IC curves for the mass numbers $m/z = 18$ (H_2O^+), 27 (HCN^+), 44 (CO_2^+), 52 ($C_2N_2^+$).
- (b) Evolution of the phase composition of $K_3[Fe(CN)_6]$ samples tempered under N_2 at twelve temperatures between 25 and 1100 °C in 100 K steps.
- (c) Three characteristic reaction stages at ca. 300, 700, and 1100 °C, respectively, are visualized by their Mößbauer spectra.

Figure 2

Simplified reaction scheme of the redox processes occurring in in the systems $K_3[Fe(CN)_6]$, $K_3[Fe(CN)_6] / AlOOH$ und $Fe^0 / AlOOH$. The reaction sequence supports and extends the mechanism proposed in [12].

Figure 3

- (a) TA-MS curves of the sample {30 % $K_3[Fe(CN)_6]$ + 70 % $AlOOH$ } (8 h co-milled) using mechanically pre-activated (50 h milling, **3**) $AlOOH$. The IC curves for the mass numbers $m/z = 12$ (C^+) and 27 (HCN^+) represent HCN, whereas $m/z = 52$ ($C_2N_2^+$) proves practically the absence of dicyane.
- (b) Mößbauer spectrum of the residue of the TA heating run in (a). The Fe component is composed from: 1 Singlet (22.5 %): $\delta = -0.056$ mm/s; $\Gamma = 0.399$ mm/s; 1 Sextet (62.1 %): $\delta = 0.018$ mm/s; $\Delta = -0.009$ mm/s; $B_{hf} = -33.07$ T; 1 Sextet (15.4 %): $\delta = 0.186$ mm/s; $\Delta = -0.001$ mm/s; $B_{hf} = -20.84$ T.

Figure 4

Mechanical activation and thermal treatment of the samples of $K_3[Fe(CN)]_6$ (**1**) and $AlOOH$ (**2**) in different gas atmospheres

Figure 5

Reference systems: Co-milling of $AlOOH$ xerogels (**2**) with 1 wt-% doping by different iron compounds as pretreatment for the TA heating runs up to 1200 °C in various gas atmospheres. The phase compositions of the samples after heating comprise compounds of Fe^0 , Fe^{2+} , and Fe^{3+} in different structural environments, among them magnetite (M) and hematite in two forms (H_a , H_b).

Table 1

Peak temperatures T_P (in °C) of the crystallization peaks of α -Al₂O₃ in the DTA heating curves in different gas atmospheres together with the percentage of decrease ΔT_P as a result of the milling or co-milling of the AlOOH xerogel with different dopants (1 wt-% each)

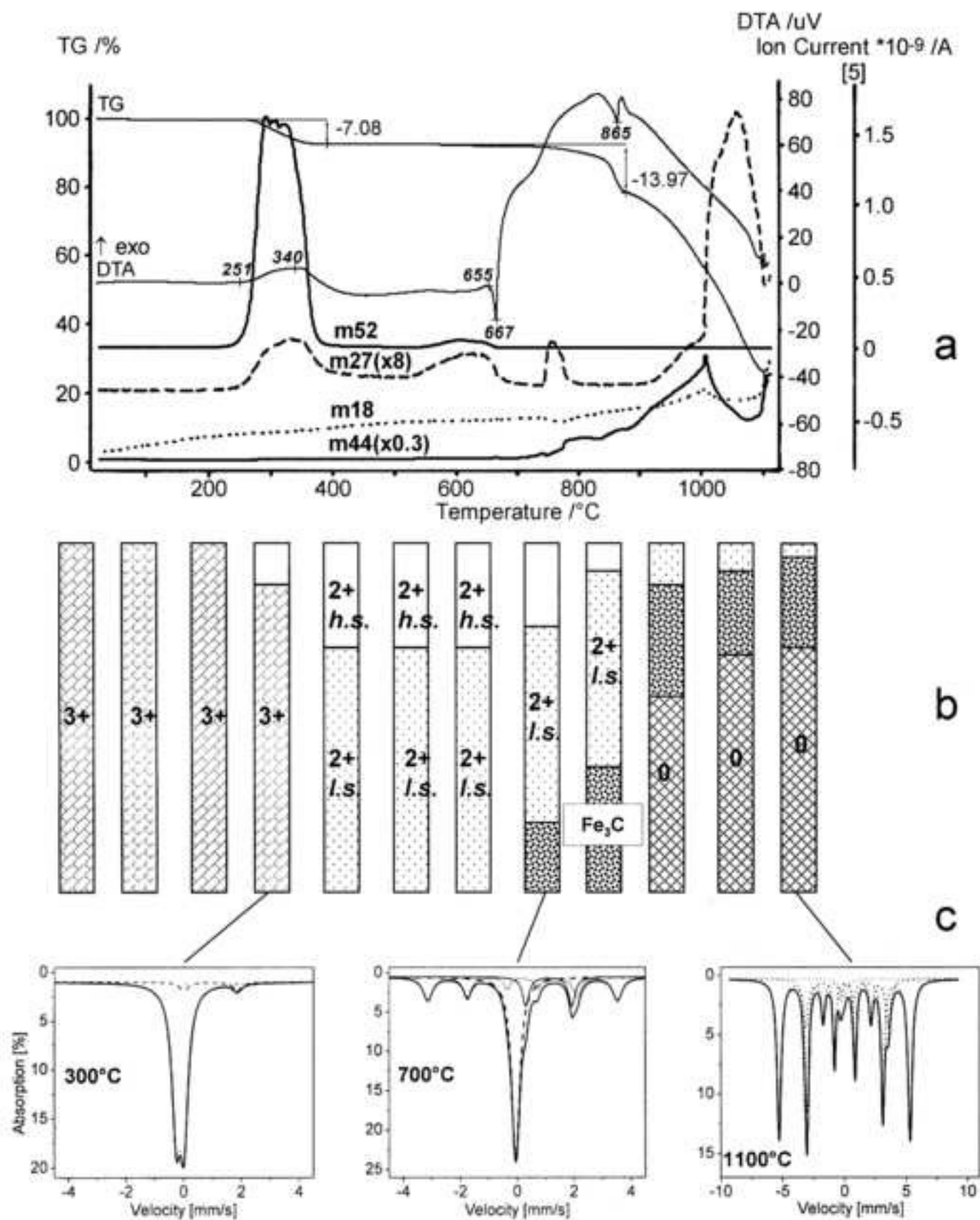
Sample	T_P / ΔT_P		
	Atmosphere during TA heating run		
	N ₂	N ₂ /O ₂	N ₂ /H ₂
AlOOH xerogel, untreated	1176	1160	1178
AlOOH xerogel, 8 h milled	1050 / -11 %	1048 / -10 %	1041 / -12 %
AlOOH xerogel, co-milled with K ₃ [Fe(CN) ₆]	1146 / -3 %	1149 / -1 %	1144 / -3 %
... co-milled with Fe(NO ₃) ₃ · 9 H ₂ O	1039 / -12 %	1038 / -11 %	1070 / -9 %
... co-milled with Al(NO ₃) ₃ · 9 H ₂ O	1083 / -7,8 %	1083 / -7 %	1090 / -9 %
... co-milled with Fe(acac) ₃	1054 / -10 %	-	-
... co-milled with Fe ₂ O ₃	987 / -16 %	-	-
... co-milled with FeCl ₃	1073 / -9 %	1082 / -7 %	1070 / -9 %
... co-milled with Fe ⁰	1070 / -9 %	1058 / -9 %	1100 / -7 %

Mechanically activated $K_3[Fe(CN)_6] / AlOOH$ forms Fe-doped AlO_x phases after heating.

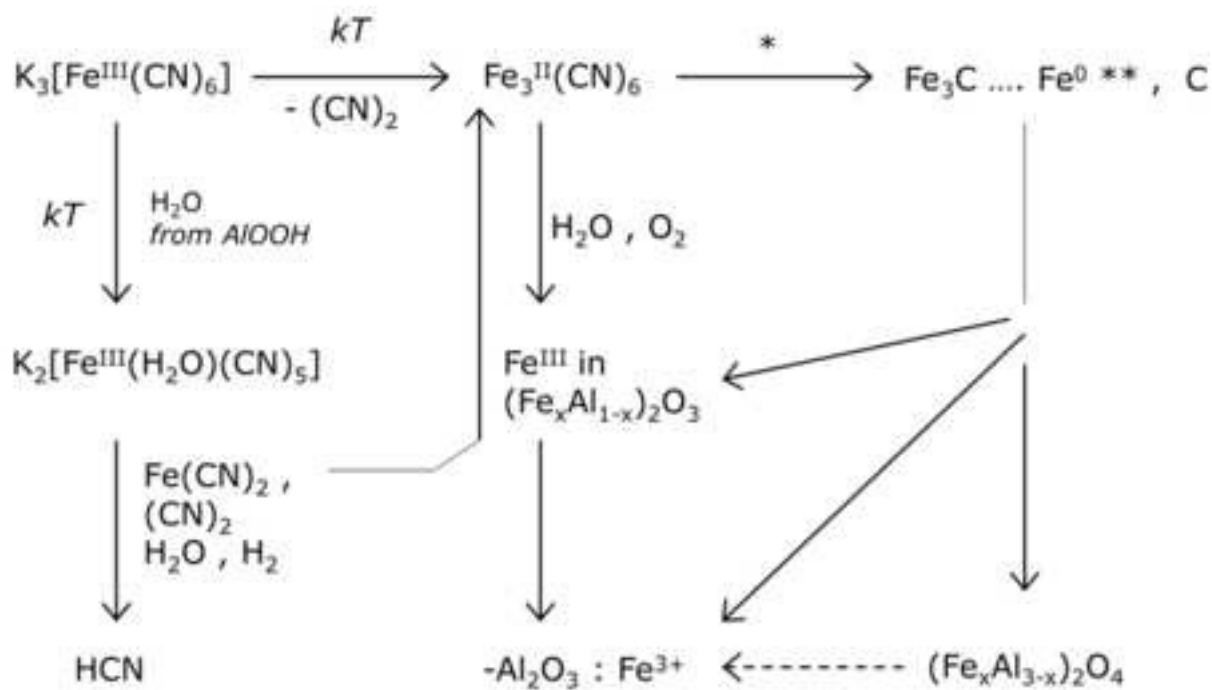
The Fe content is governed both by gas atmosphere and chemical nature of the dopant.

The formed AlO_x matrix exhibits both oxidative and protective properties.

Accepted manuscript

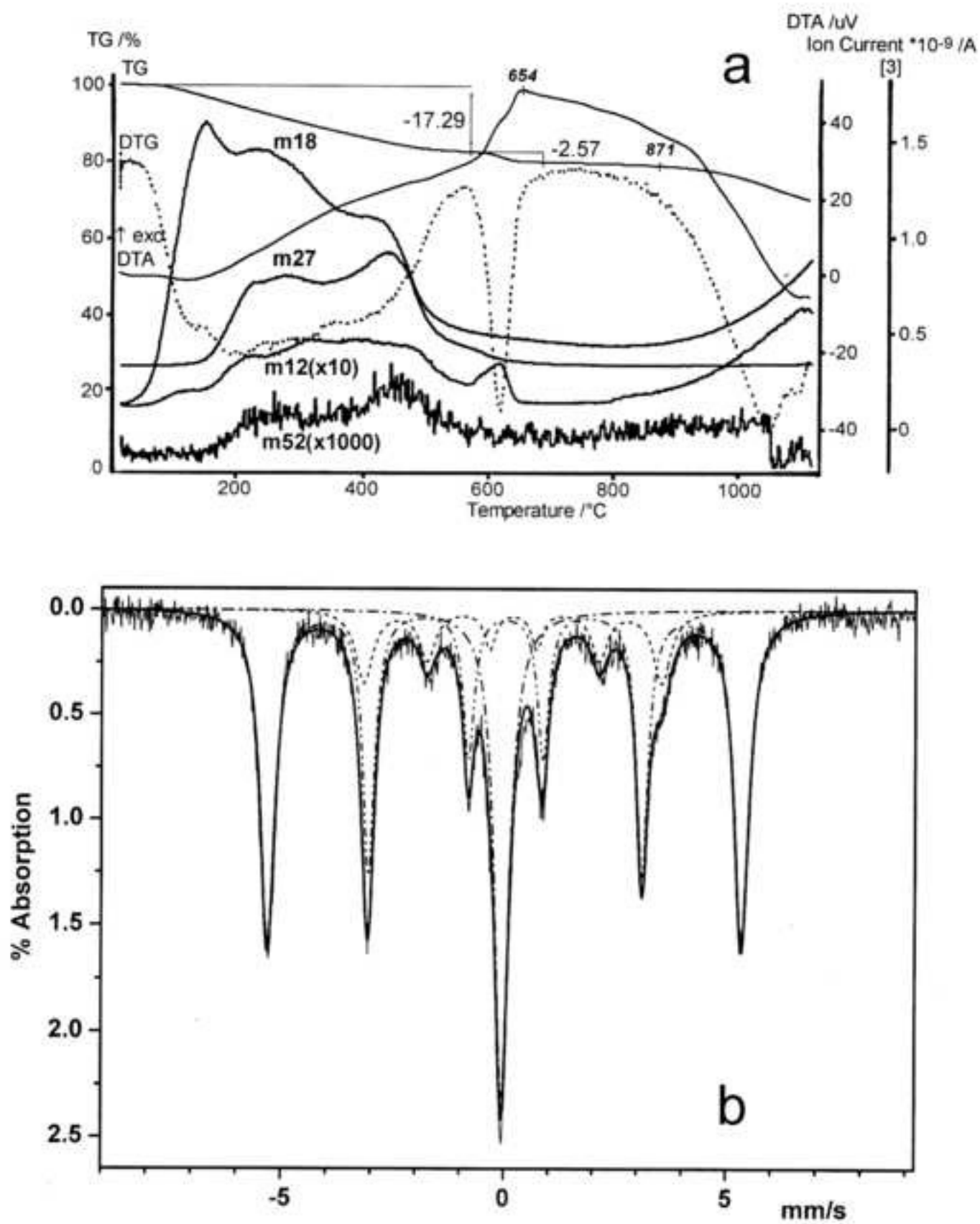


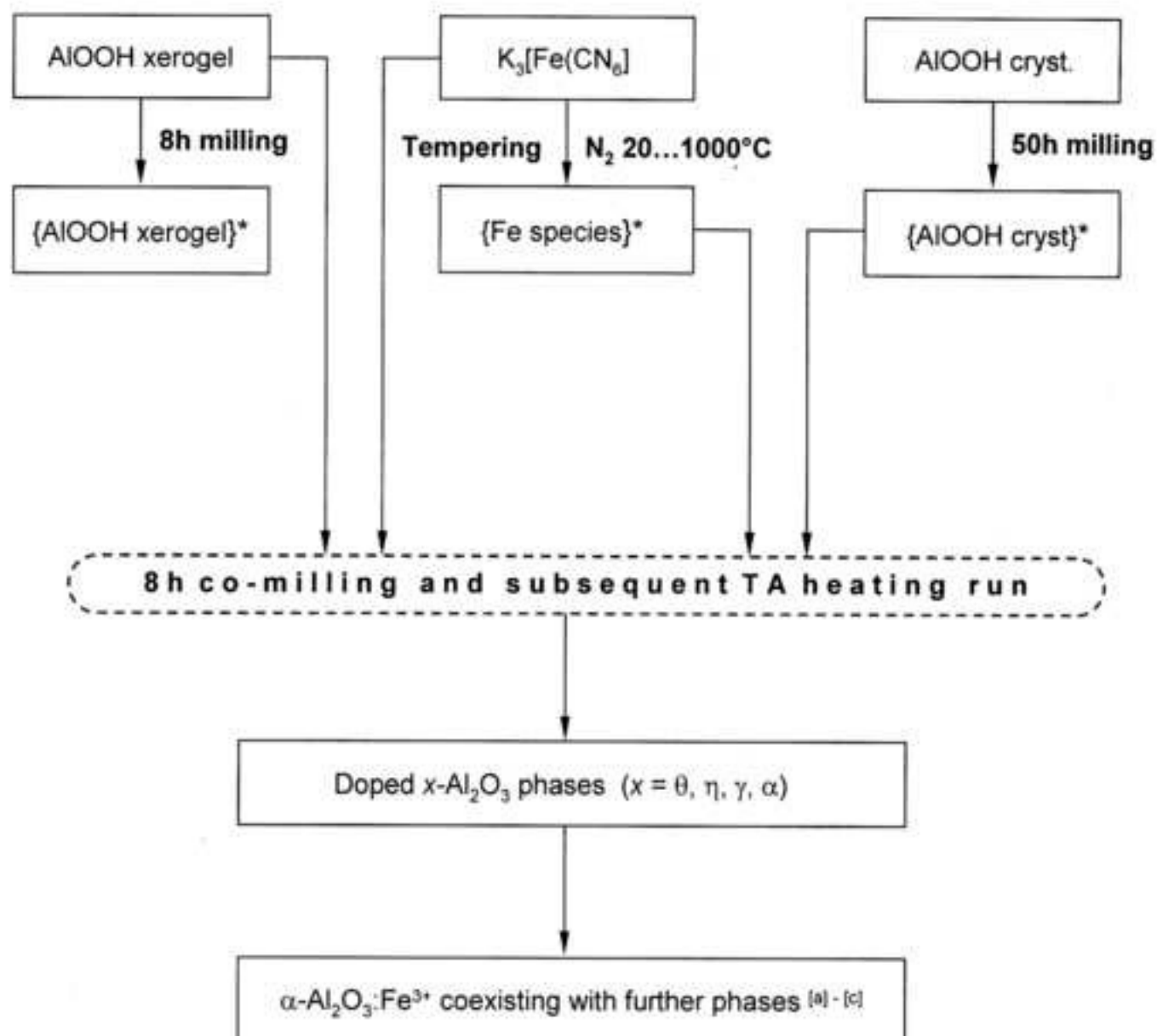
The „self-reduction“ of $K_3[Fe(CN)_6]$



- * (1) $2 K_3[Fe^{III}(CN)_6] \rightarrow 6 KCN + 2 Fe^{II}(CN)_2 + (CN)_2$
 (2) $4 KCN + Fe^{II}(CN)_2 \rightarrow K_4[Fe^{II}(CN)_6]$
 (3) $K_3[Fe^{III}(CN)_6] + Fe^{II}(CN)_2 \rightarrow KFe^{III}[Fe^{II}(CN)_6] + 2 KCN$
 (4) $3 Fe^{II}(CN)_2 \rightarrow Fe^{II}_2[Fe^{II}(CN)_6]$
 (5) $3 Fe^{II}(CN)_2 \rightarrow Fe_3C + N_2 + 5 C$
 (6) $Fe_3C \rightarrow 3 Fe + C$

** Fe^0 originating from self-reduction of $K_3[Fe^{III}(CN)_6]$
 or from externally added Fe

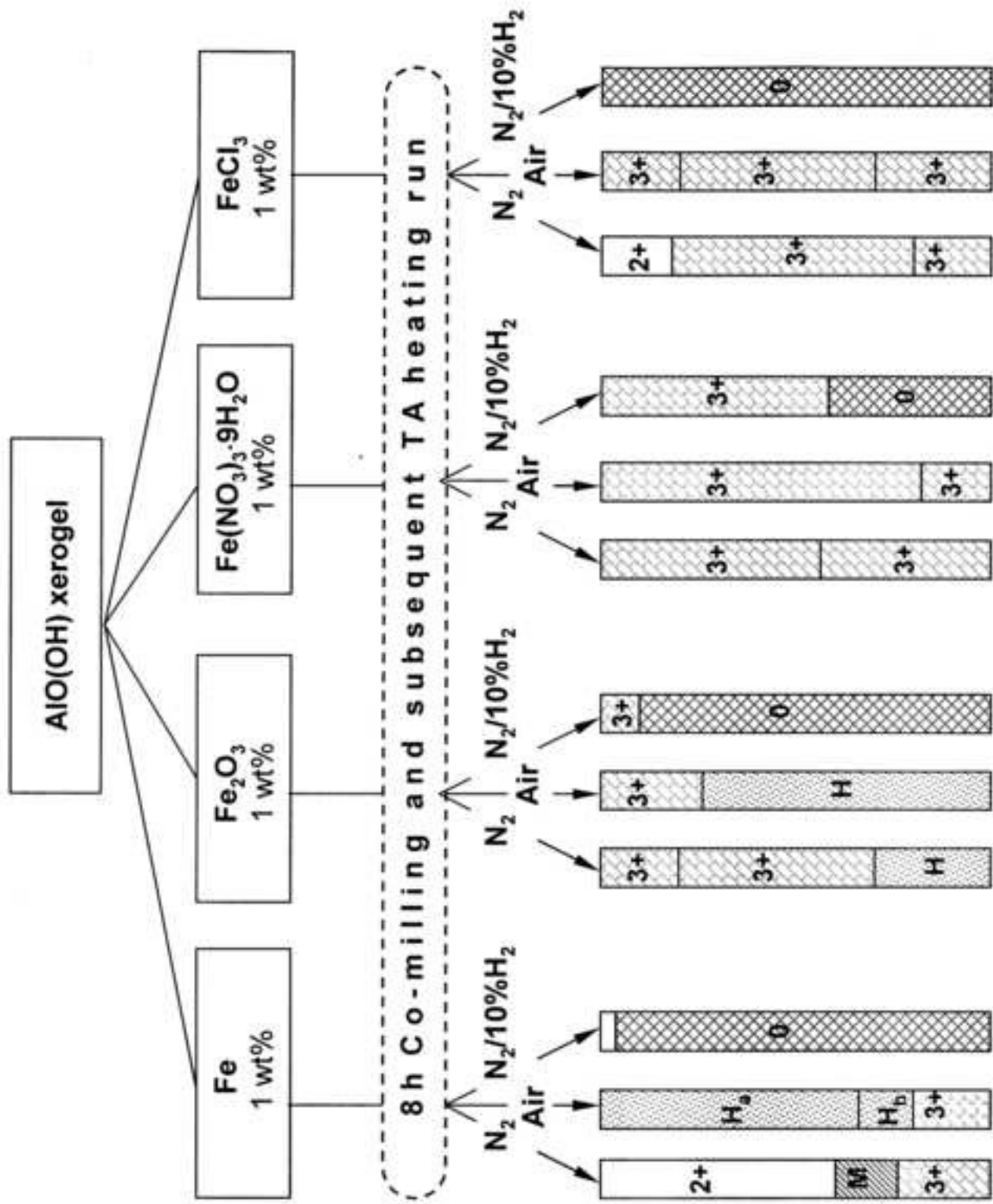




(a) Fe(0); Fe₃C

(b) Phases of the hematite row: Al₂O₃ .. (Fe_xAl_{1-x})₂O₃ .. Fe₂O₃

(c) Phases of the ferrite row: FeO·Al₂O₃ .. (Fe_{3-x}Al_x)O₄ .. Fe₃O₄



Figure(s)